Published in final edited form as:

Hum Mutat. 2016 September ; 37(9): 893–897. doi:10.1002/humu.23028.

Ehlers-Danlos Syndrome Caused by Biallelic *TNXB* Variants in Patients with Congenital Adrenal Hyperplasia

Wuyan Chen[1,*], **Ashley F. Perritt**[2,*], **Rachel Morissette**[2], **Jennifer L. Dreiling**[3], **Markus-Frederik Bohn**[4], **Ashwini Mallappa**[2], **Zhi Xu**[5], **Martha Quezado**[3], and **Deborah P. Merke**[2,6]

[1]Prevention Genetics, Marshfield, WI, USA

[2]National Institutes of Health Clinical Center, Bethesda, MD, USA

[3]Laboratory of Pathology, National Cancer Institute, Bethesda, MD, USA

[4]Department of Pharmaceutical Chemistry, University of California San Francisco, San Francisco, CA, USA

[5]National Institutes of Health, National Institute on Aging, Baltimore, MD, USA

[6]The *Eunice Kennedy Shriver* National Institute of Child Health and Human Development, Bethesda, MD, USA

Abstract

Some variants that cause autosomal recessive congenital adrenal hyperplasia (CAH) also cause hypermobility type Ehlers-Danlos syndrome (EDS) due to the monoallelic presence of a chimera disrupting two flanking genes: *CYP21A2*, encoding 21-hydroxylase, necessary for cortisol and aldosterone biosynthesis, and *TNXB*, encoding tenascin-X, an extracellular matrix protein. Two types of CAH tenascin-X (CAH-X) chimeras have been described with a total deletion of *CYP21A2* and characteristic *TNXB* variants. CAH-X CH-1 has a *TNXB* exon 35 120bp deletion resulting in haploinsufficiency and CAH-X CH-2 has a *TNXB* exon 40 c.12174C>G (p.Cys4058Trp) variant resulting in a dominant-negative effect. We present here three patients with biallelic CAH-X and identify a novel dominant-negative chimera termed CAH-X CH-3. Compared with monoallelic CAH-X, biallelic CAH-X results in a more severe phenotype with skin features characteristic of classical EDS. We present evidence for disrupted tenascin-X function and computational data linking the type of tenascin-X to disease severity.

Keywords

congenital adrenal hyperplasia; Ehlers-Danlos syndrome; tenascin-X; CAH-X; biallelic

Approximately 9% of patients with autosomal recessive congenital adrenal hyperplasia (CAH) due to 21-hydroxylase deficiency (CAH; MIM# 201910) have CAH-X, a connective

Corresponding author: Dr. Deborah P. Merke, M.D., M.S., National Institutes of Health Clinical Center, Bldg 10, Rm 1-2740, 10 Center Drive, Bethesda, MD 20892-1932, USA, dmerke@nih.gov.

*These authors contributed equally to this work.

Clinical Trial Registration Number: ClinicalTrials.gov Identifier #NCT00250159

tissue dysplasia due to a contiguous deletion affecting *CYP21A2* (MIM# 613815) and *TNXB* (MIM# 600985) on one allele (Morissette, et al., 2015). *CYP21A2* encodes 21-hydroxylase, an essential enzyme in the biosynthesis of cortisol and aldosterone, and CAH due to 21-hydroxylase deficiency results in cortisol and aldosterone deficiency and androgen excess (Speiser, et al., 2010). Flanking the *CYP21A2* gene is *TNXB*, which encodes the extracellular matrix (ECM) glycoprotein tenascin-X (TNX) that is involved in collagen organization and matrix integrity (Egging, et al., 2007). Variants in *TNXB* have been associated with Ehlers-Danlos syndrome (EDS) (Merke, et al., 2013; Morissette, et al., 2015; Schalkwijk, et al., 2001).

EDS is a heterogeneous group of disorders characterized by connective tissue fragility with a clinical spectrum ranging from mild to life-threatening. The 1998 Villefranche classification of EDS (Beighton et al 1998) defined 6 subtypes with major and minor diagnostic criteria. The classical subtype major criteria are a triad of marked skin hyperextensibility, widened atrophic scars and joint hypermobility, with minor criteria reflecting features consistent with connective tissue weakness such as easy bruising and hernias. Classical EDS is typically autosomal dominant and is associated with type V collagen deficiency (De Paepe and Malfait, 2012). Hypermobility type EDS is the mildest EDS subtype with generalized joint hypermobility, recurrent joint dislocations and chronic arthralgias can occur, and mild skin manifestations such as smooth, velvety skin may also be present. The genetic etiology of hypermobility type EDS is largely unknown (De Paepe and Malfait, 2012; Sobey, 2014). In this report, we describe a subtype of EDS in CAH patients with biallelic *TNXB* variants that clinically resembles the classical type EDS phenotype. Prior studies of patients with CAH and monoallelic *TNXB* variants reported a phenotype similar to the hypermobility type EDS (Merke, et al., 2013; Morissette, et al., 2015).

Two types of chimeric genes, designated CAH-X CH-1 and CAH-X CH-2, have been identified to cause CAH-X syndrome, the presence of EDS in a patient with autosomal recessive CAH: CAH-X CH-1 involves the 120bp deletion in the exon 35 region of *TNXB* and leads to haploinsufficiency (Merke, et al., 2013; Morissette, et al., 2014); CAH-X CH-2 involves the c.12174C>G (p.Cys4058Trp) variant in exon 40 of *TNXB*, which does not alter TNX expression but rather causes a dominant-negative effect due to the loss of a critical disulfide bond in the TNX fibrinogen-like domain (Morissette, et al., 2015). In CAH-X CH-2, the c.12174C>G (p.Cys4058Trp) variant was previously reported by our group to sometimes co-segregate with a cluster of three pseudogene-derived variants of uncertain significance [exon 41: c.12218G>A (p.Arg4073His); exon 43: c.12514G>A (p.Asp4172Asn) and c.12524G>A (p.Ser4175Asn)] (Morissette, et al., 2015). We now present evidence that the cluster of these three variants alone likely causes structural changes to the TNX protein, resulting in an EDS clinical phenotype and identification of a novel dominant-negative chimera, CAH-X CH-3.

This study was carried out at the National Institutes of Health Clinical Center in Bethesda, MD (Clinical Trials #NCT00250159) with approval from the *Eunice Kennedy Shriver* National Institute of Health & Human Development Institutional Review Board. All participants and parents of participating children gave written informed consent and minors 8 years or older gave assent. *CYP21A2* and *TNXB* genotyping, and EDS clinical evaluations

were done as previously reported (Morissette, et al., 2015). The reference sequences for *TNXB* are NM_019105.6 (mDNA) and NP_061978.6 (protein); the reference sequences for *CYP21A2* are NM_000500.7 (mDNA) and NP_000491.4 (protein). For missense variants, Alamut Visual (Version 2.7, April 2015; Interactive Biosoftware, http://www.interactive-biosoftware.com/alamut-visual/) was used for the individual variant analyses, providing computational algorithms for SIFT (Ng and Henikoff, 2001) (Version 1, http://sift.jcvi.org/) and PolyPhen-2 (Adzhubei, et al., 2010) (Version 2.2.2, 2012, http://genetics.bwh.harvard.edu/pph2/).

Three patients, ages 19, 14 and 29 years old with CAH, presented with a more severe EDS phenotype than the monoallelic forms of CAH-X. All three patients demonstrated a unique combination of *TNXB* variants on both alleles (Figure 1A). Except for the father of Proband 1 (P1), five parents were genotyped and the origins of the variants found in the probands were revealed. P1 is heterozygous for the c.12174C>G (p.Cys4058Trp) variant and homozygous for the three variant cluster [exon 41: c.12218G>A (p.Arg4073His); exon 43: c.12514G>A (p.Asp4172Asn) and c.12524G>A (p.Ser4175Asn)], CAH-X CH-3 (Figure 1B). Proband 2 (P2) was previously reported to be heterozygous for the 120bp deletion (CAH-X CH-1, which was inherited from the mother) (Merke, et al., 2013), but upon further genetic testing has the c.12174C>G (p.Cys4058Trp) variant and the three variant cluster on the paternal allele (Figure 1B). Proband 3 (P3) is homozygous for the c.12174C>G (p.Cys4058Trp) variant and no other notable variants were found (Figure 1B). All variants presented are located in the C-terminal fibrinogen-like domain of TNX. The four individual missense TNXB variants described in this manuscript have been submitted to the ClinVar database (http://www.ncbi.nlm.nih.gov/clinvar/).

Our three patients fulfilled all major diagnostic criteria for classical type EDS: skin hyperextensibility (Figure 1C1–3), widened atrophic scars (Figure 1C4) and joint hypermobility (Figure 1C5) (Beighton, et al., 1998). All three patients had significant joint hypermobility (Beighton score ≥ 7). P1 and P3 had extreme joint laxity with a history of joint dislocations, chronic arthralgias and chronic tendonitis and/or bursitis. P1 had multiple unstable joints that spontaneously dislocated with routine activities of daily life, such as walking. Other clinical findings included piezogenic pedal papules (Figure 1C6, P1, P2 and P3), elongated uvula with or without midline crease (P1 and P2), rectal prolapse (P1 and P2), severe gastroesophageal reflux (P2), high palate (P3), and pes planus (P1 and P3). Cardiac abnormalities included mild ventricular enlargement in P1 and P3.

All three patients with biallelic CAH-X had skin laxity and widened scars. Patients with monoallelic CAH-X due to CAH-X CH-1 had mostly joint hypermobility with little to no skin findings (Merke, et al., 2013), while approximately one-half of patients with CAH-X due to CAH-X CH-2 had skin laxity (Morissette, et al., 2015). Moreover, one patient (P1) self-reported delayed wound healing. Interestingly, our patients with biallelic CAH-X also displayed more skin abnormalities than the five patients previously reported by Schalkwijk et al. (2001) with autosomal recessive EDS due to tenascin deficiency (Schalkwijk, et al., 2001). Although these EDS patients reported by Schalkwijk, et al. had hyperelastic skin, wound healing and scar formation were reported as normal. The effect of having an endocrine disorder on the EDS phenotype is unknown.

Five of six parents were available for genotyping and had fewer clinical findings than their children. The father of P1 was unavailable for study. The mother of P1 (heterozygous for p.Cys4058Trp with cluster) had chronic elbow tendonitis and hyperextensible knees and fingers. The father of P2 (heterozygous for p.Cys4058Trp) had hyperextensible fingers and right knee, and cardiac MRI revealed a mildly enlarged right ventricle and mild biatrial enlargement. The mother of P2 (heterozygous for exon 35 120bp deletion) had hypermobile large and small joints and chronic arthralgia. The father of P3 (heterozygous for p.Cys4058Trp) did not report EDS findings, although the mother (heterozygous for p.Cys4058Trp) reported generalized hypermobility. These results are consistent with our previous findings of CAH-X CH-1 and CAH-X CH-2 carriers having varied and milder phenotypes than patients concomitantly affected by CAH.

We performed immunohistochemical and histology staining of dermal biopsies from probands and controls as previously reported for monoallelic CAH-X (Morissette, et al., 2015), with the addition of Masson Trichrome for collagen fibers. Compared to healthy controls and monoallelic CAH-X patients, all three patients displayed reduced elastic fiber formation by van Gieson's staining, with a distinct lack of fibers perpendicular to the dermis. In addition, marked reduction in horizontal fiber organization in the deep dermis was observed in P1 (Figure 2A). These results more closely resemble the CAH-X CH-2 rather than the haploinsufficient CAH-X CH-1 findings, though elastin appears to be more affected overall in the biallelic dermis (Morissette, et al., 2015). Fibrillin-1 immunohistochemical staining revealed shortened (P2 and P3) and disorganized (P3) fibers compared to monoallelic CAH-X and healthy controls (Figure 2A). P1 and P2 staining resembled that shown in our CAH-X CH-2 cohort (Morissette, et al., 2015), while P3 fibers were highly disorganized. Masson Trichrome staining for overall collagen was done using an Artisan Multistainer (DakoCytomation, Carpinteria, CA, USA) and Dako Artisan staining reagents (Masson Trichrome Kits, DakoCytomation). The epidermal layer served as an internal negative control for each skin biopsy. Trichrome staining revealed reduced collagen density in all three cases when compared to both healthy controls and monoallelic CAH-X patients; however, P1 and P2 were much more reduced than P3 (Figure 2A). Overall, P1 shows the most disrupted staining pattern of all three cases, consistent with his phenotype having the most significant skin and joint findings. Fibrillin-1 and overall collagen density were less impaired in P3 who does not carry the three variant cluster. These data suggest that the three variant cluster present in P1 and P2 may impact the TNX protein and its ability to function in the ECM more than having the p.Cys4058Trp variant alone.

We previously showed that the p.Cys4058Trp variant characteristic of CAH-X CH-2 leads to the loss of a critical disulfide bond in the tertiary structure of the TNX C-terminal fibrinogen-like domain (Morissette, et al., 2015). In order to explore the role that the associated three variant cluster may be playing in TNX and its function, we modeled the TNX fibrinogen-like domain using Prime (Schrödinger, LLC, New York, NY, USA) (Jacobson, et al., 2004) for knowledge-based homology modeling and PDB ID: 2J3F as a template structure. The resulting model was energy minimized using the "Protein Refinement" module with the OPLS2005 force field (Banks, et al., 2005). The three variants in the cluster were generated, energy minimized, and the thermodynamic stability analyzed using the BioLuminate package (Schrödinger, LLC) (Salam, et al., 2014). Figures were

generated using PyMOL (Schrödinger, LLC). Figure 2B (left) shows the TNX fibrinogen-like domain (*green*) with p.Cys4058 and the variant cluster [p.Arg4073, p.Asp4172 and p.Ser4175] as sticks (*orange*). Energy minimized models reveal how p.Cys4058Trp and p.Arg4073His interfere with domain stability. p.Arg4073 is predicted to form a cation-pi interaction (*red* oval) with p.Phe4080 (Figure 2B, top right), which is lost in the p.Arg4073His change, penalizing the folding energy with a loss of 35 kcal/mol. The amino acid substitution prediction programs PolyPhen-2 (Adzhubei, et al., 2010) and SIFT predicted the p.Arg4073His change to be “probably damaging” and “deleterious”, respectively. More severe changes appear after introducing p.Cys4058Trp (Figure 2B, bottom right), which disrupts a highly conserved internal disulfide bond and likely affects proper folding of secondary structure (*purple* oval), as previously reported (Morissette, et al., 2015). The loss in interaction energy in this mutant is 58 kcal/mol. The remaining variants in the cluster did not significantly affect the folding energies in the models. Therefore, modeling and energy calculations suggest that both the p.Cys4058Trp and p.Arg4073His variants are detrimental to proper TNX folding, and that further destabilization of the TNX protein occurs if both are present. Homozygosity for the p.Arg4073His variant may explain the observed severe effects in the skin and ECM of P1. To date, no patients have been identified who are homozygous for both the p.Cys4058Trp variant and the cluster of three variants, but likely this combination would lead to an even more dysfunctional TNX protein. A possible consequence of this involves TGF-β bioavailability. Alcaraz et al. showed that a direct interaction exists between the FBG domain and the latent TGF-β complex (Alcaraz, et al., 2014). They also showed that FBG-induced activation of latent TGF-β requires the cell surface adhesion receptor integrin α11β1 and cell adhesion to the FBG domain was critical for TGF-β activation. Therefore, disrupted cell adhesion in this region would likely prevent normal TGF-β activation and function. We hypothesize that the unfolded TNX protein, likely through the p.Cys4058Trp and p.Arg4073His variants, would interfere with proper cell adhesion, leading to disrupted TGF-β binding and further downstream effects in the ECM.

CAH-X has been reported to have an autosomal dominant mode of inheritance, and three chimeric forms have now been identified, including the CAH-X CH-1 (Merke, et al., 2013), CAH-X CH-2 (Morissette, et al., 2015) and the novel CAH-X CH-3 presented here. While CAH-X CH-1 is known to lead to haploinsufficiency, both CAH-X CH-2 and CAH-X CH-3 most likely result in a dominant-negative effect due to missense substitutions. Our data presented here and in prior studies support specific phenotype-genotype correlations. First, compared to haploinsufficiency, a dominant-negative affect causes a more severe phenotype displayed by greater skin and joint involvement (Morissette, et al., 2015). Second, the dosage of dominant alleles correlates with the severity of the phenotype. An even greater disruption of elastic and fibrillin-1 fibers was found in the biallelic CAH-X patients compared with that of the monoallelic CAH-X CH-2 patients, suggesting a co-dominant like effect of biallelic *TNXB* missense variants. Third, an accumulative effect of missense variants on the same allele may result in a more severe phenotype. Further studies with a larger sample size are needed to evaluate this effect.

This study describes a biallelic form of CAH-X syndrome that is clinically and biochemically more severe than the monoallelic forms previously described (Merke, et al.,

2013; Morissette, et al., 2015). We have chosen to use the terminology “biallelic”, rather than “autosomal recessive” to describe our CAH patients with *TNXB* variants on both alleles because the term “autosomal recessive” by definition implies that having a deleterious variant on one allele does not result in a clinical phenotype. Clearly this is not the case with CAH-X. Similarly, biallelic variants of well-established autosomal dominant disorders resulting in a more severe phenotype have been described in polycystic kidney disease (Bergmann, et al., 2011; Hopp, et al., 2012; Sandford, 2009), familial hypercholesterolemia (Varret, et al., 2008) and inherited cancers (Rahman and Scott, 2007). Thus, our findings reflect complex genetic heterogeneity not unexpected.

The strength of this study is the combination of biochemical experiments, computational modeling and extensive phenotyping data collected and the large cohort size of patients affected by CAH. We are limited by the current data available on the tenascin-X gene and protein, and the lack of an appropriate CAH-X mouse model. However, the development of *in vitro* constructs for probing variants in TNX and the effect on its mechanism of action would provide useful functional information. Another avenue to consider was recently reviewed by Valcourt, et al., where TNX was discussed as a matricellular, rather than just an architectural protein (Valcourt, et al., 2015). TNX has been shown to modulate cell adhesion; (Alcaraz, et al., 2014) therefore, examining TNX’s signaling function in the context of its matricellular properties opens the door for a new means of studying this extracellular matrix glycoprotein.

This study reveals that CAH-X syndrome exists in a wide spectrum of inheritance modes, including the monoallelic and biallelic forms. The severity of the phenotype is dependent on the carriership of *TNXB* variants, as the allelic heterogeneity of this cohort demonstrates. Modeling and computational analyses of the TNX protein revealed the effects these variants are likely having on the protein’s ability to properly fold and function in the ECM. Studying the mechanistic role of each newly identified variant will shed light on this poorly understood structural protein that is so critical for connective tissue integrity. Likely, the known prevalence of CAH-X will increase as more TNX variants and *TNXA/TNXB* chimeric genes are discovered. As the phenotypic spectrum of CAH-X widens, greater care in evaluating CAH patients for EDS features is warranted. Moreover, expanding our understanding of EDS through studies of extracellular matrix genes and extensive phenotyping of patients emphasizes the need for reclassification of EDS in order to capture these novel connective tissue dysplasias.

Acknowledgments

Funding: This work was supported by the Intramural Research Programs of the National Institutes of Health Clinical Center, the *Eunice Kennedy Shriver* National Institute of Child Health and Human Development, the National Cancer Institute, and the National Institute on Aging.

The authors thank the patients for their study participation. D. Merke is a Commissioned Officer in the United States Public Health Service. D. Merke received unrelated research funds from Diurnal Limited, Ltd. through an NIH Cooperative Research and Development Agreement.

REFERENCES

Adzhubei IA, Schmidt S, Peshkin L, Ramensky VE, Gerasimova A, Bork P, Kondrashov AS, Sunyaev SR. A method and server for predicting damaging missense mutations. Nature methods. 2010; 7(4): 248–249. [PubMed: 20354512]

Alcaraz LB, Exposito JY, Chuvin N, Pommier RM, Cluzel C, Martel S, Sentis S, Bartholin L, Lethias C, Valcourt U. Tenascin-X promotes epithelial-to-mesenchymal transition by activating latent TGF-beta. J Cell Biol. 2014; 205(3):409–428. [PubMed: 24821840]

Banks JL, Beard HS, Cao Y, Cho AE, Damm W, Farid R, Felts AK, Halgren TA, Mainz DT, Maple JR, et al. Integrated Modeling Program, Applied Chemical Theory (IMPACT). J Comput Chem. 2005; 26(16):1752–1780. [PubMed: 16211539]

Beighton P, De Paepe A, Steinmann B, Tsipouras P, Wenstrup RJ. Ehlers-Danlos syndromes: revised nosology, Villefranche, 1997. Ehlers-Danlos National Foundation (USA) and Ehlers-Danlos Support Group (UK). Am J Med Genet. 1998; 77(1):31–37. [PubMed: 9557891]

Bergmann C, von Bothmer J, Ortiz Brüchle N, Venghaus A, Frank V, Fehrenbach H, Hampel T, Pape L, Buske A, Jonsson J, et al. Mutations in Multiple PKD Genes May Explain Early and Severe Polycystic Kidney Disease. Journal of the American Society of Nephrology : JASN. 2011; 22(11): 2047–2056. [PubMed: 22034641]

De Paepe A, Malfait F. The Ehlers–Danlos syndrome, a disorder with many faces. Clinical Genetics. 2012; 82(1):1–11. [PubMed: 22353005]

Egging D, van Vlijmen-Willems I, van Tongeren T, Schalkwijk J, Peeters A. Wound healing in tenascin-X deficient mice suggests that tenascin-X is involved in matrix maturation rather than matrix deposition. Connect Tissue Res. 2007; 48(2):93–98. [PubMed: 17453911]

Hopp K, Ward CJ, Hommerding CJ, Nasr SH, Tuan H-F, Gainullin VG, Rossetti S, Torres VE, Harris PC. Functional polycystin-1 dosage governs autosomal dominant polycystic kidney disease severity. The Journal of Clinical Investigation. 2012; 122(11):4257–4273. [PubMed: 23064367]

Jacobson MP, Pincus DL, Rapp CS, Day TJ, Honig B, Shaw DE, Friesner RA. A hierarchical approach to all-atom protein loop prediction. Proteins. 2004; 55(2):351–367. [PubMed: 15048827]

Merke DP, Chen W, Morissette R, Xu Z, Van Ryzin C, Sachdev V, Hannoush H, Shanbhag SM, Acevedo AT, Nishitani M, et al. Tenascin-X haploinsufficiency associated with Ehlers-Danlos syndrome in patients with congenital adrenal hyperplasia. J Clin Endocrinol Metab. 2013; 98(2):E379–E387. [PubMed: 23284009]

Morissette R, Chen W, Perritt AF, Dreiling JL, Arai AE, Sachdev V, Hannoush H, Mallappa A, Xu Z, McDonnell NB, et al. Broadening the Spectrum of Ehlers Danlos Syndrome in Patients With Congenital Adrenal Hyperplasia. J Clin Endocrinol Metab. 2015; 100(8):E1143–E1152. [PubMed: 26075496]

Morissette R, Merke DP, McDonnell NB. Transforming growth factor-beta (TGF-beta) pathway abnormalities in tenascin-X deficiency associated with CAH-X syndrome. Eur J Med Genet. 2014; 57(2–3):95–102. [PubMed: 24380766]

Ng PC, Henikoff S. Predicting Deleterious Amino Acid Substitutions. Genome Research. 2001; 11(5): 863–874. [PubMed: 11337480]

Rahman N, Scott RH. Cancer genes associated with phenotypes in monoallelic and biallelic mutation carriers: new lessons from old players. Human Molecular Genetics. 2007; 16(R1):R60–R66. [PubMed: 17613548]

Salam NK, Adzhigirey M, Sherman W, Pearlman DA. Structure-based approach to the prediction of disulfide bonds in proteins. Protein Eng Des Sel. 2014; 27(10):365–374. [PubMed: 24817698]

Sandford RN. The diversity of PKD1 alleles: implications for disease pathogenesis and genetic counseling. Kidney Int. 2009; 75(8):765–767. [PubMed: 19337214]

Schalkwijk J, Zweers MC, Steijlen PM, Dean WB, Taylor G, van Vlijmen IM, van Haren B, Miller WL, Bristow J. A recessive form of the Ehlers-Danlos syndrome caused by tenascin-X deficiency. N Engl J Med. 2001; 345(16):1167–1175. [PubMed: 11642233]

Sobey G. Ehlers–Danlos syndrome – a commonly misunderstood group of conditions. Clinical Medicine. 2014; 14(4):432–436. [PubMed: 25099849]

Speiser PW, Azziz R, Baskin LS, Ghizzoni L, Hensle TW, Merke DP, Meyer-Bahlburg HF, Miller WL, Montori VM, Oberfield SE, et al. Congenital adrenal hyperplasia due to steroid 21-hydroxylase deficiency: an Endocrine Society clinical practice guideline. J Clin Endocrinol Metab. 2010; 95(9): 4133–4160. [PubMed: 20823466]

Valcourt U, Alcaraz LB, Exposito JY, Lethias C, Bartholin L. Tenascin-X: beyond the architectural function. Cell Adh Migr. 2015; 9(1–2):154–165. [PubMed: 25793578]

Varret M, Abifadel M, Rabès JP, Boileau C. Genetic heterogeneity of autosomal dominant hypercholesterolemia. Clinical Genetics. 2008; 73(1):1–13. [PubMed: 18028451]

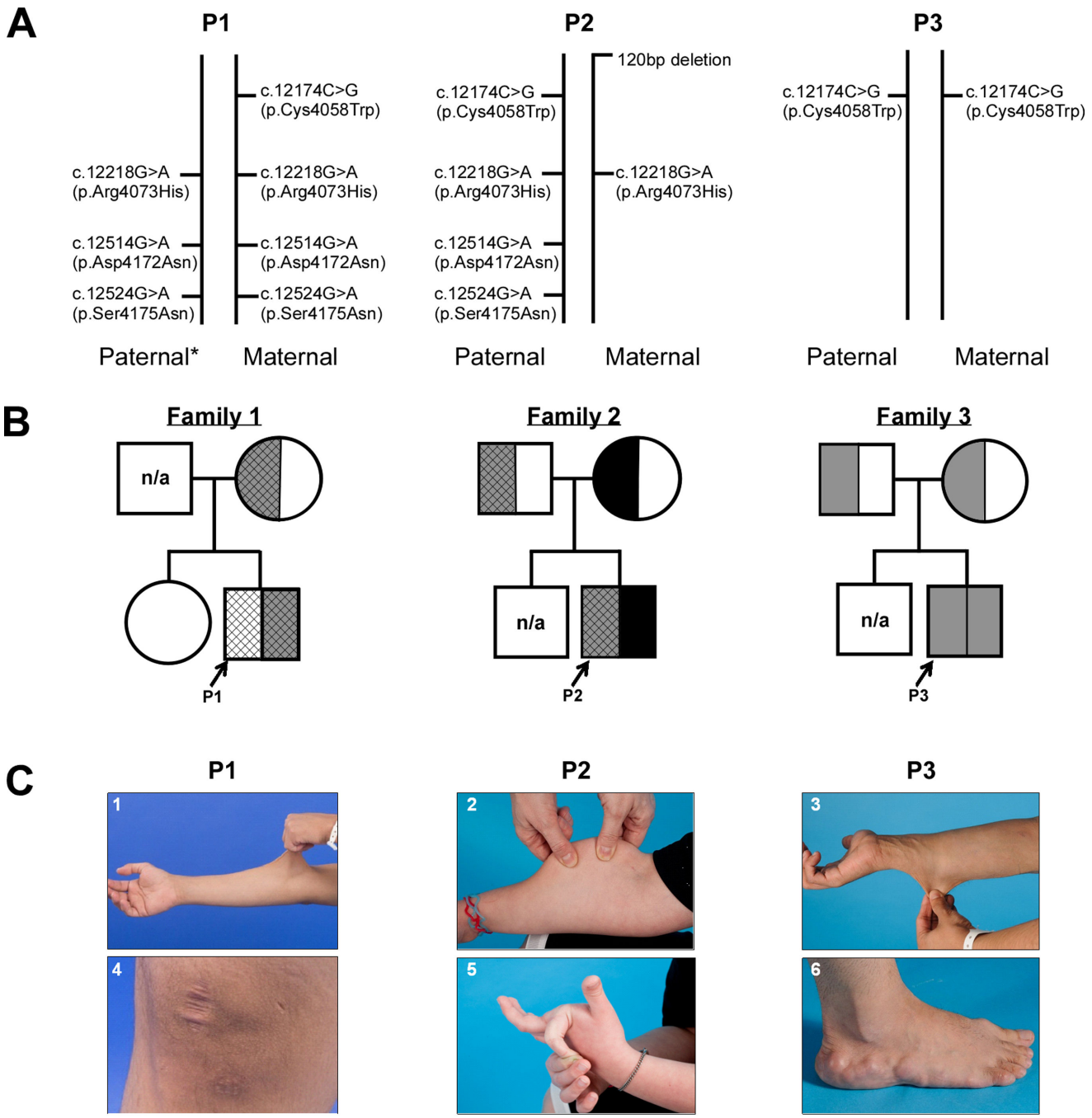

Figure 1.

Biallelic CAH-X Genetics and Phenotypes **A**: *TNXB* variants found on the paternal and maternal alleles of each proband. *: presumed, not available for testing. **B**: Pedigrees of biallelic CAH-X families. Black represents CAH-X CH-1 (exon 35 120bp deletion). Grey represents CAH-X CH-2 [c.12174C>G (p.Cys4058Trp) as hallmark]. Cross-hatched lines represent the presence of the three variant cluster [exon 41: c.12218G>A (p.Arg4073His); exon 43: c.12514G>A (p.Asp4172Asn) and c.12524G>A (p.Ser4175Asn)]. n/a: not

available. **C:** Clinical findings in probands with biallelic CAH-X. Skin laxity (1, 2, 3), wide scars (4), hypermobile joints (5), and piezogenic pedal papules (6) were found.

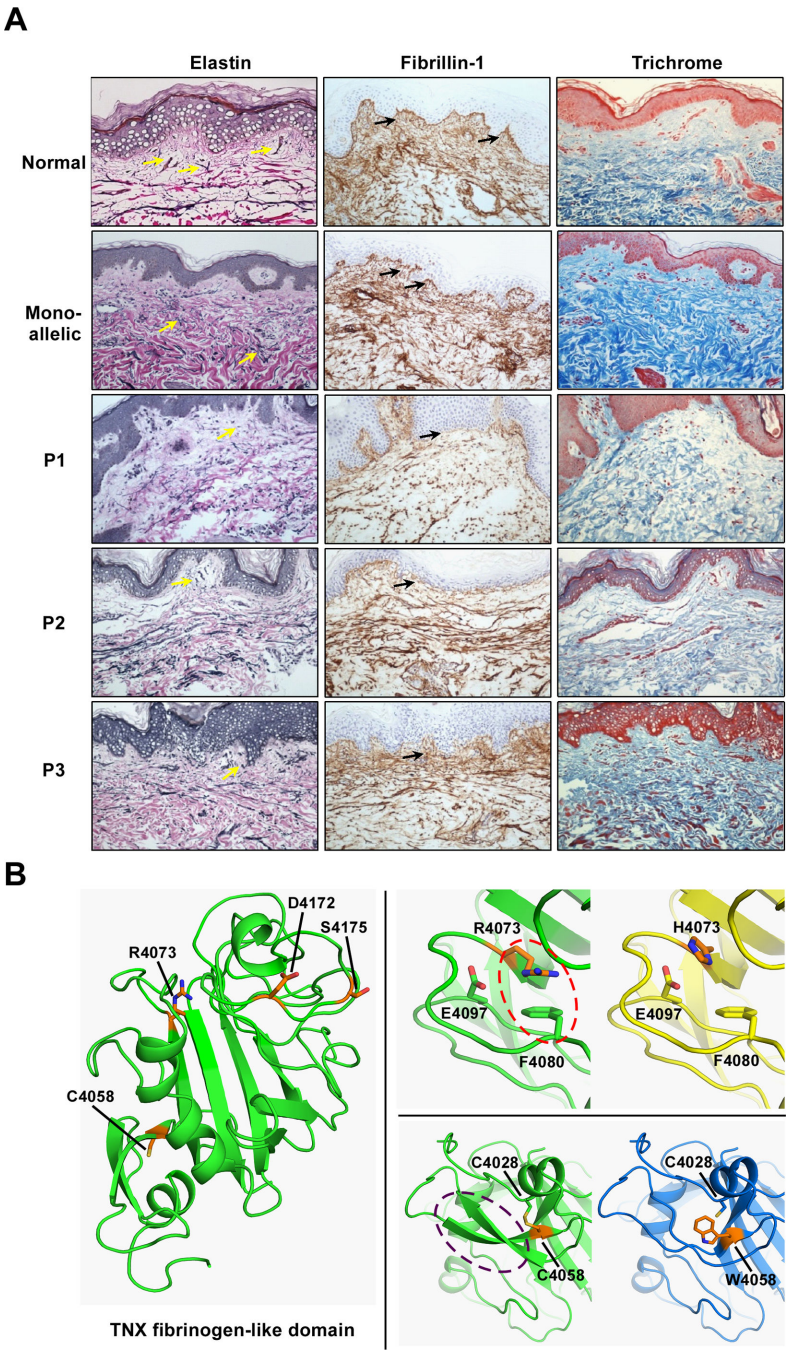

Figure 2.

The Effect of Biallelic CAH-X on the Extracellular Matrix. **A:** Representative staining of extracellular matrix markers in dermal tissue of three biallelic CAH-X patients compared to monoallelic patients and healthy controls reveal reduced van Gieson's staining of elastic fibers (yellow arrows), shortened (P1, P2) and disorganized (P3) fibrillin-1 fibers (black arrows) by immunohistochemical staining, and reduced overall collagen density by Masson Trichrome staining of collagen fibers. Hematoxylin and eosin were used to counterstain and sections were viewed at 200× magnification. **B:** Model of the TNX fibrinogen-like domain

(cartoon, *green*) with p.Cys4058 (C4058) and the variant cluster [p.Arg4073 (R4073), p.Asp4172 (D4172) and p.Ser4175 (S4175)] shown as sticks (*orange*). Energy minimized models of single residue mutants reveal how p.Cys4058Trp (C4058W) and p.Arg4073His (R4073H) interfere with domain stability. p.Arg4073 (R4073) is predicted to form a cation-pi interaction (*red* oval) with p.Phe4080 (F4080), which is lost in the p.Arg4073His (R4073H) change, penalizing the folding energy with a loss of 35 kcal/mol. More severe changes appear after introducing p.Cys4058Trp (C4058W), which disrupts a highly conserved internal disulfide bond and likely affects proper folding of secondary structure (*purple* oval). The loss in interaction energy in this mutant is 58 kcal/mol.